New technique of self-refilling friction stir welding to repair keyhole

L. Zhou*[1,2], D. Liu[1,2], K. Nakata[1], T. Tsumura[1], H. Fujii[1], K. Ikeuchi[1], Y. Michishita[3], Y. Fujiya[3] and M. Morimoto[4]

A new technique of self-refilling friction stir welding (SRFSW) relying on non-consumable joining tool has been developed to repair the keyhole left at the end of 316L stainless steel friction stir welding/friction stir processing (FSW/FSP) seam. The conventional FSW process was transformed by adopting a series of non-consumable tools with gradual change in geometry to create a solid state refilled joint step by step. Using the combined plastic deformation and flow of the material around the keyhole, the SRFSW process is able to repair the keyhole with both metallurgical and mechanical bonding characteristics, and the FSW/FSP seam can be achieved without keyhole or other obvious macro defects. Microstructural observation results showed that the grains in the refilled zone were significantly refined by the tool. Tensile test results showed the refilled joint fractured at the base metal side, and the relative tensile strength and elongation are 112 and 82% of the base metal respectively. Moreover, no sigma phase but few Cr carbides were found in the refilled zone, which would not result in obvious corrosion resistance degradation of 316L stainless steel.

Keywords: Self-refilling friction stir welding, Austenitic stainless steel, Keyhole, Non-consumable tool, Repairing

Introduction

Friction stir welding (FSW) is a novel solid state joining technique invented by The Welding Institute in 1991.[1] In typical FSW, a non-consumable rotating tool with a specially designed pin is inserted into the abutting edges of the plates to be joined and moves along the joint line. The material is softened and flows around the rotating pin under a combined effect of frictional and plastic deformation heating and thus forming a solid state bonding between the two workpieces. It is energy efficient, environment friendly and versatile and thus is considered to be the most remarkable development for materials joining in the past two decades. Until now, FSW has been successfully applied to weld various aluminium, magnesium and copper alloys. In recent years, FSW of high melting temperature materials such as steels and titanium alloys has become a research hotspot, and enormous progress has been made.[2–5] However, it has been known that welding defects may be formed during the FSW process when improper welding parameters or technological conditions are used,[6–11] and such defects as groove, cavity and kissing bond have significant influence on the mechanical properties of the joints.[12–18] Particularly, keyhole remains at the end of the weld inevitably, resulting from the extraction of a general non-consumable pin after welding, which could be the weakest part of the joint. As for the defects such as groove, cavity and kissing bond, the re-FSW process is proposed, but the keyhole would emerge again when these defects are repaired.[19] In a sense, the problems caused by the remained keyhole can be solved by leaving it in the runoff plate, but this method is limited to structures in many cases, while repairing method by fusion welding technology results in significant decrease of joint performance.

To repair the keyhole in FSW welds, a lot of methods and apparatuses have been developed. Engineers of the National Aeronautics and Space Administration have developed an autoadjusting pin tool apparatus, which could be used for materials of varying thickness, and the pin can be incrementally withdrawn from the workpieces during the final stage of the transverse, thus eliminating the exit keyhole in the weld.[20] Furthermore, the retractable[21] or double acting refilling tool,[22] consisting of separated outer shoulder and inner pin, has been developed to eliminate the remained keyhole for FSW by controlling the relative movement of shoulder and pin at the final stage of welding. Friction taper plug welding (FTPW) or friction hydro pillar processing (FHPP) is a solid state joining process developed by The Welding Institute during the 1990s, which involves drilling a tapered through hole into a plate. Subsequently, a tapered

[1]Joining and Welding Research Institute, Osaka University, 11-1 Mihogaoka, Ibaraki, Osaka 567-0047, Japan
[2]Shandong Provincial Key Laboratory of Special Welding Technology, Harbin Institute of Technology at Weihai, Weihai 264209, China
[3]Manufacturing Technology Center, Mitsubishi Heavy Industries, Ltd, Takasago 676-8686, Japan
[4]ITER Superconducting Magnet Technology Group, Division of ITER Project, Japan Atomic Energy Agency, Naka 311–0193, Japan

*Corresponding author, email zhouli@hitwh.edu.cn

Published by Maney on behalf of the Institute
Received 25 June 2012; accepted 30 July 2012
DOI 10.1179/1362171812Y.0000000058

Table 1 Chemical compositions and mechanical properties of 316L stainless steel plates

Chemical compositions/mass-%									Mechanical properties	
C	Si	Mn	P	S	Ni	Cr	Mo	Fe	Strength/MPa	Elongation/%
0·009	0·66	1·06	0·034	0·005	12·15	17·52	2·07	Bal.	531	61

plug with a similar included angle is friction welded to the matching surface of the hole in a few seconds by forcing the rotating plug against the drilled hole.[23,24] It can be used in several applications, for example, at the location of a defect or crack in offshore steel and aerospace aluminium structures that is intended to be repaired,[25,26] and probably can be extended to repair the remained keyholes in friction stir welds. Recently, a new technique called filling friction stir welding (FFSW) has been proposed by Huang *et al.*[27,28] based on the basic principle of FTPW/FHPP, where a semiconsumable tool consists of non-consumable shoulder, and consumable joining bit is designed to repair the keyholes in aluminium alloy FSW welds. Compared with the FTPW/FHPP process, excess sections of the plug could be cut automatically under proper tool design and process parameters during the FFSW.

The named auto-adjusting or retractable or double acting FSW tools must be installed on exceedingly complex and expensive equipment. Especially, it is difficult to realise the system for the high melting point materials due to limitations of pin tool materials and thus tool design. As for the FTPW/FHPP process, it has been demonstrated to be an effective way to repair defects like keyhole. However, a tapered through hole and proper plug should be prepared to get defect free joints, especially for high melting point material thick structures due to the high flow stress. In our previous work, austenitic stainless steel 316L as modified grades of AISI type 316, which has applications as structural material for the construction of water storage tanks in nuclear power plants, was friction stir processed using polycrystalline cubic boron nitride (PCBN) tools to repair stress corrosion cracking for extending the service life of water storage tanks.[29,30] As further investigation of the previous study, efforts have been made to repair the remained keyhole on the friction stir processed 316L plates. However, there exist obvious macro defects at the bottom of the refilled keyhole when the FFSW process without geometry changes to the blind keyhole was adopted, which can be attributed to insufficient plasticisation due to the low heat conductivity and high plastic deformation resistance of stainless steel, while the preparation of a specific through hole for FTPW/FHPP is not desirable due to the limitations of the actual working environment. In view of this, a new technique of self-refilling friction stir welding (SRFSW) is proposed in the present work, where conventional FSW process was transformed by adopting a series of non-consumable tools with gradual change in geometry, and the keyhole is refilled by combined plastic deformation and flow of the material around the keyhole using the designed tools step by step. Furthermore, microstructural evolution and mechanical properties of the refilled joint are investigated in detail.

Experimental

The base metal (BM) was $200 \times 150 \times 10$ mm 316L stainless steel plate with the chemical compositions and mechanical properties shown in Table 1. Friction stir processing (FSP) was performed using the PCBN tool, and the related details were given in our previous reports.[29,30] To repair the keyhole, a series of PCBN tools for SRFSW were designed with gradual change in geometry of pin diameter and pin length, as listed in Table 2. Similar to the tool for FSP, convex shoulder with spiral pattern surface was designed for SRFSW tools to enhance the stirring effect. The SRFSW process was carried out using the specially designed tools step by step, and the surrounding keyhole material was heated by friction and plasticisation, and then squeezed into the keyhole. Finally, the keyhole was self-repaired without adding other filler metal, as illustrated by Fig. 1. The FSP and SRFSW processes were performed on a load controlled FSW machine, and argon shielding was employed around the tool during the process to avoid surface oxidation. The parameters of FSP/SRFSW and corresponding keyhole appearance after each step are summarised in Table 3. These parameters for the FSP/SRFSW process were determined based on preparatory experiments, in which several welding parameters, the tool rotation speed ω, applied force F and welding speed V or holding time T, were tried including the tool design.

The refilled joint was examined by metallurgical inspections performed on the transverse (perpendicular to the original FSP direction) cross-section of the joint. Microstructural evolution was examined by optical microscopy (Keyence VHX-200/100F), scanning electron microscopy (SEM; Keyence VE-8800) and

Table 2 Tool geometries and features for FSP and SRFSW

Process	Tool code	Tool geometry	Shoulder diameter/mm	Pin diameter at tip/mm	Pin length/mm	Pin conicity/°
FSP	FSP	Threaded conical pin	22	4	5	30
SFFSW	SRFSW-1	Threaded conical pin	22	4·3	5	30
	SRFSW-2	Threaded conical pin	22	5·4	4·6	30
	SRFSW-3	Threaded conical pin	22	7·2	4·2	30
	SRFSW-4	Threaded conical pin	22	10·1	4	30
	SRFSW-5	Threaded conical pin	22	13·0	3·7	30
	SRFSW-6	Threaded conical pin	22	14·8	3·3	30
	SRFSW-7	Threaded conical pin	22	0	1·9	80
	SRFSW-8	Only shoulder	22	…	…	…

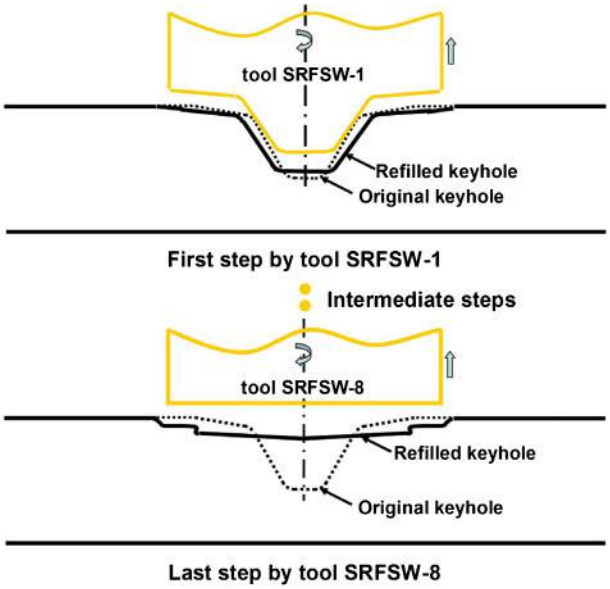

1 Schematic illustration for SRFSW process

transmission electron microscopy (TEM; Hitachi HF2000). The transverse joint cross-section was cut by electrical discharge machining and prepared by standard metallographic procedures. The polished joint cross-section was electrolytically etched in a solution of 10% oxalic acid + 90% water with a power supply set to 15 V and 6 mA mm^{-2} for 90 s and then observed on the optical microscope and through SEM. Thin discs for TEM were cut from the various locations of the joint cross-section using a focussed ion beam instrument (SII SMI3050MS2) and were observed on the TEM at 200 kV. Vickers hardness along the transverse joint centreline was measured every 1 mm spacing on an Akashi AAV-500 Vickers hardness tester using a load of 0·98 N for 15 s. Transverse tensile test sample with geometric details according to JIS Z2201 shown in Fig. 2 was cut perpendicularly from the joint obtained with the same process parameters for metallurgical inspections with the top and bottom surfaces eliminated. Tensile test was carried out on an Instron 5500 mechanical tester at room temperature using a crosshead speed of 1 mm min^{-1}.

Results and discussion

A macroscopic overview of the cross-section of the refilled joint by SRFSW is presented in Fig. 3. It can be seen that the refilled joint without obvious macro defects can be obtained when appropriate tool design and process parameters are carried out. The typical refilled zone (RZ), thermomechanically affected zone (TMAZ) and BM are observed. However, the RZ consists of several layers (Fig. 3), which is caused by the multistep SRFSW process in our case. Moreover, it should be noted that banded structures, similar to that in the

Table 3 Process parameters for FSP/SRFSW and keyhole appearance after each step

Experimental No.	Tool code	Process parameter ω–*F*–*V* (FSP)/ω–*F*–*T* (SRFSW)	Keyhole appearance after each step
1	FSP	300 rev min^{-1}–30 kN–20 mm min^{-1}	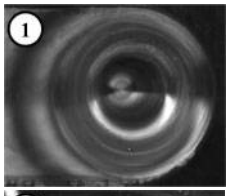
2	SRFSW-1	1200 rev min^{-1}–30 kN–5 s	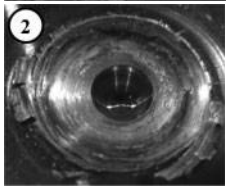
3	SRFSW-2	1200 rev min^{-1}–30 kN–5 s	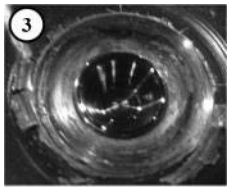
4	SRFSW-3	1200 rev min^{-1}–30 kN–5 s	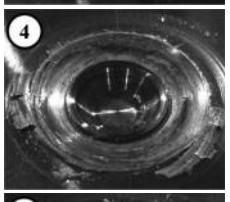
5	SRFSW-4	1200 rev min^{-1}–30 kN–5 s	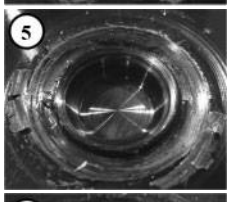
6	SRFSW-5	1500 rev min^{-1}–30 kN–5 s	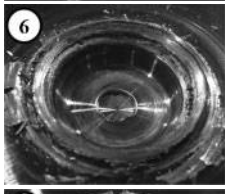
7	SRFSW-6	1500 rev min^{-1}–30 kN–5 s	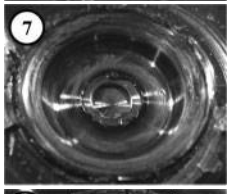
8	SRFSW-7	1500 rev min^{-1}–30kN–5 s	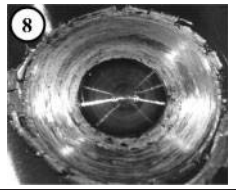
9	SRFSW-8	1500 rev min^{-1}–30 kN–5 s	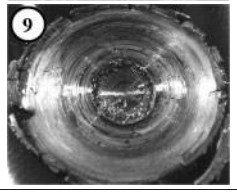

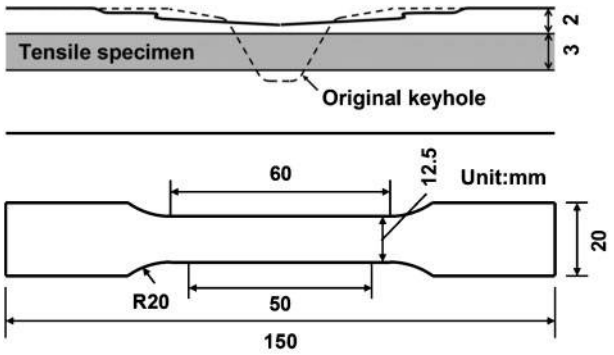

2 Schematic illustration for tensile specimen

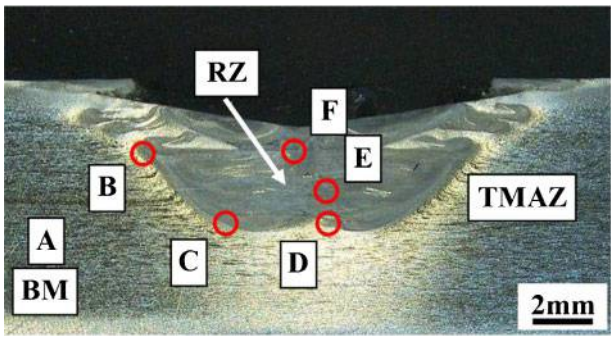

3 Transverse cross-section appearance of refilled joint by SRFSW

friction stir processed zone of 316L stainless steel,[29,30] are detected in the RZ. In our case, the authors are mainly interested in the microstructural feature in typical areas of the RZ in the refilled joint, and thus, several characteristic positions (positions B–F shown in Fig. 3) in the RZ and in the BM (position A shown in Fig. 3) are observed.

The details of the microstructural variations are demonstrated in Fig. 4. It can be seen from Fig. 4*a* that the BM consists of coarsened grain structures in the range of 30–80 μm distributed along the rolling direction of the plate. Figure 4*b–d* shows the microstructure in the RZ as well as in the surrounding TMAZ from the upper part to the bottom of the refilled keyhole. It is indicated that excellent metallurgical and mechanical bonding is obtained between the RZ and the TMAZ. The typical band structure mentioned above can be seen in the RZ near the TMAZ, which is characterised by lamellar structures that look like lineal etch pits (Fig. 4*b*) as reported in our previous study.[29,30] The TMAZ, where both the thermal and the plastic deformation effects are received during the welding, is characterised as a much refined microstructure that consists of equiaxed dynamically recrystallised grains as well as elongated deformed grains along the metal flow direction induced by stirring, as shown in Fig. 4*b–d*. Figure 4*e* and *f* shows the microstructure in the typical areas of the inner RZ, where a significantly refined equiaxed recyrstallised grain structure with average size of several micrometres is formed, which could be attributed to the severe deformation effect caused by the tool. In addition, the interfaces between different layers are formed in the multistep SRFSW process, as indicated by Fig. 4*e* and *f*. The layer interfaces in Fig. 4*e* and *f* are further examined by SEM with higher magnification, as shown in Fig. 5. It is indicated that the layer interfaces are with metallurgical and mechanical bonding characteristics, but tiny cavity or gap may exist at the interface, which could be attributed to the insufficient plasticisation caused by low heat conductivity and high plastic deformation resistance of 316L stainless steel.

Figure 6 shows the microhardness distributions, typical tensile properties and fracture locations of the refilled joint without obvious macro defects. It can be seen from Fig. 6*a* that the microhardness in the RZ is slightly higher than that of the BM, which could be attributed to microstructural refinement in the RZ during the welding process. The stress–strain curve shows a typical ductile fracture feature during the tensile test, and the tensile test sample fractures at the BM side, as shown in Fig. 6*b*; thereby, it can be concluded that the small cavity or gap at layer interfaces has no significant effect on tensile properties of the refilled joint. The tensile strength is evaluated by nominal stress, and the elongation was determined by measuring the gauge length within the reduced section before and after testing. The observed tensile test result is an average over the gauge length including various zones of the joint, and thus, there is some difference in tensile properties between the refilled joint and the BM though the refilled joint fractures at the BM side. Tensile test shows that the tensile strength of the refilled joint without obvious macro defects is slightly improved due to microstructural refinement in the RZ, which is 112% of that of the BM. However, the relative elongation is only 82% of that of the BM, which could be attributed to the plastic constraint effect in the refilled joint during the tensile test caused by microstructural evolution and thus difference in deformation capacity of different areas. The SRFSW process increases the effective cross-sectional area of the nugget, resulting in higher tensile strength and thus is qualified for repairing the keyhole.

As for processes like SRFSW based on the basic principles of FSW, the advantages result from the fact that the process takes place in the solid state below the melting point of the material to be joined, especially for the materials that are difficult to be joined by conventional fusion welding method, such as high strength aluminium alloys. However, previous studies have demonstrated that the sigma phase could be rapidly formed in the friction stir welded/friction stir processed zone of austenitic stainless steel,[29–32] which results in Cr depletion zone around the precipitates and thus will worsen the corrosion resistance of austenitic stainless steel.[33] Microstructure in typical areas of the RZ is further observed and characterised by TEM. Images (TEM) are shown in Fig. 7. No evidence of sigma phase formation is identified in the RZ, but few rod-like carbides with the size of several hundreds of nanometres along the grain boundaries are observed. Carbides in austenitic stainless steel have several types, which depend on metallurgical composition and process history. Generally, $Cr_{23}C_6$ is the most common Cr carbide in austenitic stainless steel and is given priority for formation during processing. In the present condition, the selected electron diffraction pattern for the typical positions of the RZ reveals that besides the $Cr_{23}C_6$ phase, the Cr_7C_3 phase with trigonal structure,

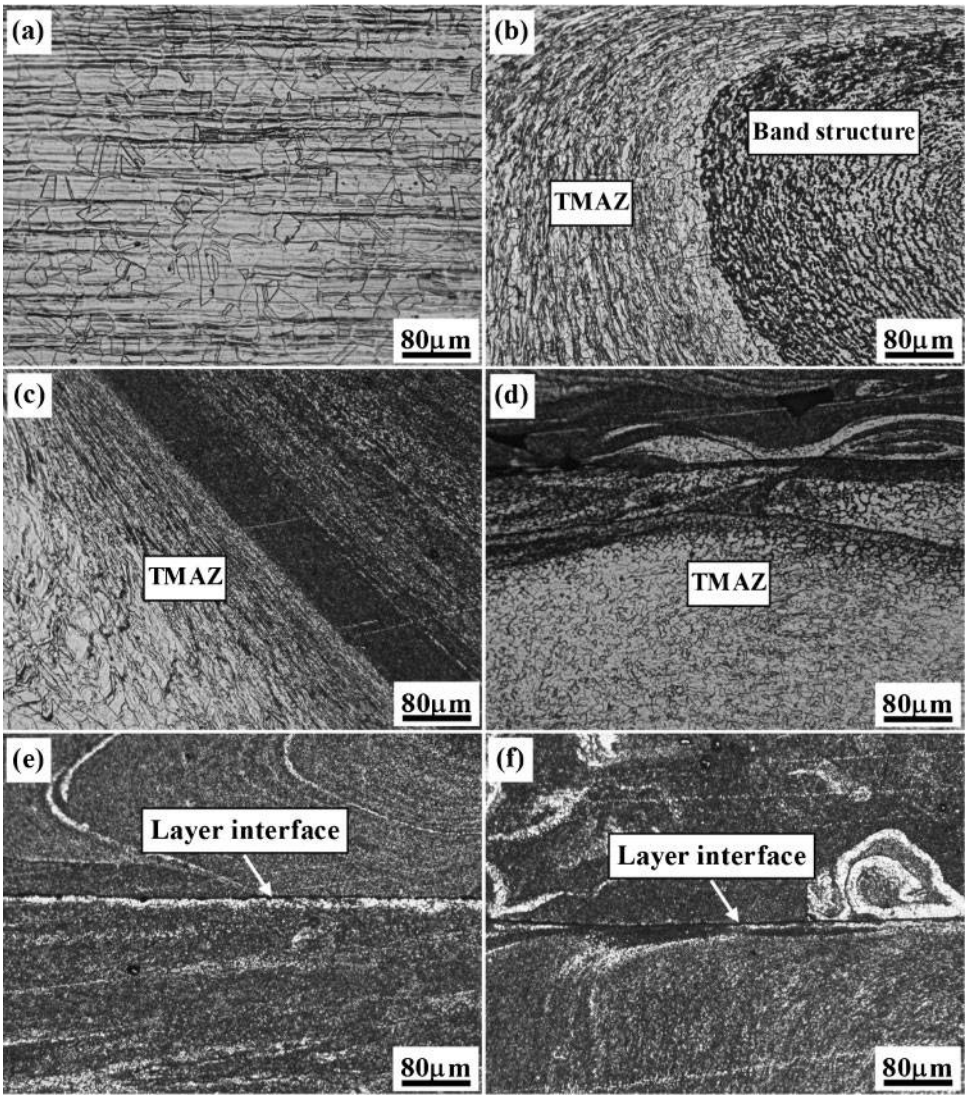

a position A; *b* position B; *c* position C; *d* position D; *e* position E; *f* position F

4 OM microstructures of different positions shown in Fig. 3

a=13·980 Å and c=4·523 Å is also formed, as indicated by Fig. 7.

In general, the sigma phase is formed in austenitic stainless steel during aging at temperatures between 773 and 1073 K. The direct decomposition of austenite to sigma phase requires a long time due to the accompanying redistribution of alloying elements by substitutional diffusion.[34] However, sigma formation can be accelerated in the duplex microstructure of ferrite and austenite phases and can be significantly accelerated by strain and recrystallisation during aging.[35,36] Since FSW introduces high strain and it accompanies dynamic recrystallisation in the stir zone, Park *et al.*[31,37] suggest that the sigma phase can be rapidly formed by the transformation of austenite to delta ferrite at high temperatures and the subsequent decomposition of the ferrite under the high strain and recrystallisation induced by friction stirring. In the current SRFSW process for 316L stainless steel,

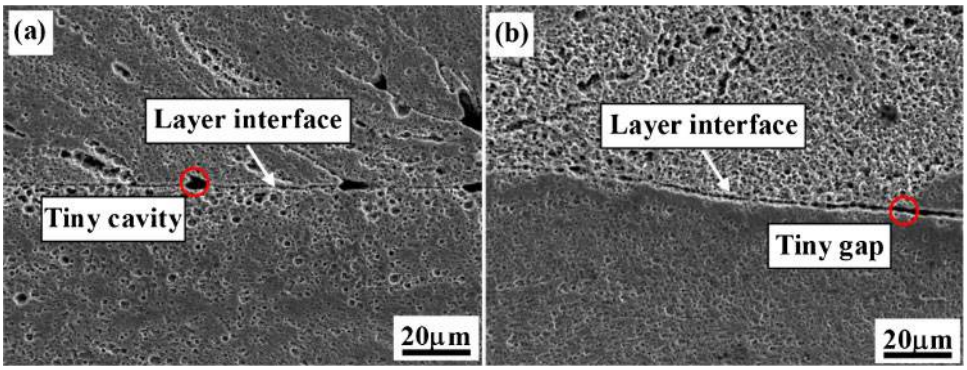

5 SEM microstructures of typical layer interfaces shown in *a* Fig. 4*e* and *b* Fig. 4*f*

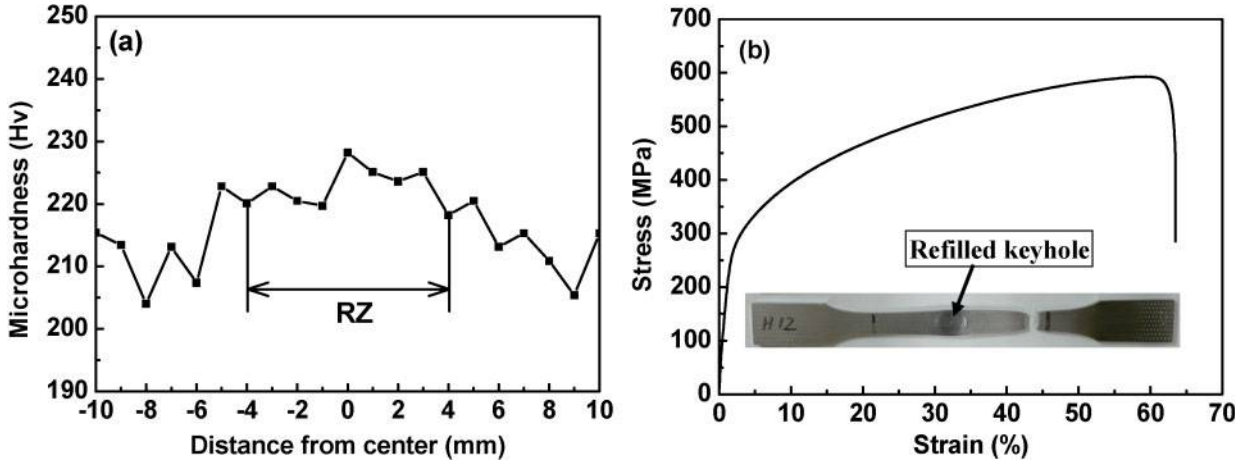

a microhardness distribution; *b* stress–strain curve of tensile test

6 Hardness profile and tensile properties of refilled joint by SRFSW method

the holding time is only 5 s for each step, and thus, the high temperature retention time is relatively short compared with that in the conventional FSW/FSP process performed at low tool travel speed, which could not provide enough time for the formation of sigma phases in the RZ. Finally, no sigma phase is formed in the RZ of 316L stainless steel SRFSW joint.

Compared with conventional fusion welding, the most attractive aspect for this novel repair technology is that the BM is not melted, and thus, the porosity and grain boundary cracking associated with fusion welding repair technology can be eliminated and the mechanical property of the repair zone can be significantly improved. Moreover, it can offer advantages for online application particularly in terms of its lower risk of through wall penetration. Meanwhile, it can also avoid preparing a specific tapered through hole into a plate like that in the FTPW/FHPP process, which provides better adaptability for the actual working condition. The precipitation of Cr carbides could cause Cr depletion and result in the degradation of the corrosion resistance of austenite stainless steel. However, the amount of Cr carbides in the RZ is very few and thus would not degrade the corrosion resistance of 316L stainless steel obviously. Therefore, SRFSW technology to repair the keyhole is a preferred online repair technology.

Conclusions

Keyholes in 316L stainless steel plates were successfully repaired by SRFSW technology using non-consumable tool. The microstructural evolution and the mechanical properties of the refilled joint were investigated. The important findings are shown as the following:

1. The refilled joint without obvious macro defects could be obtained when appropriate tool design and processing parameters were carried out. Microstructure in the RZ was significantly refined, which exhibited a roughly equiaxed grain structure with average size of several micrometres.

2. The microhardness in the RZ of the refilled joint without obvious macro defects was slightly higher than that of BM. Tensile test results showed the tensile specimen fractured at the BM side, and the relative tensile strength and elongation of the refilled joint were 112 and 82% of the BM respectively.

3. No sigma phase was detected in the RZ due to the relatively short high temperature retention time. The

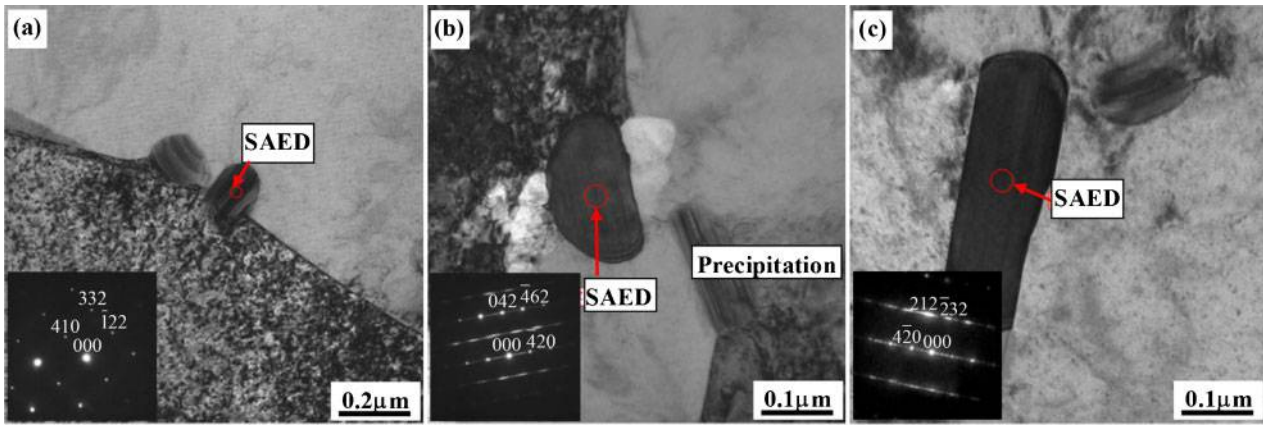

a position B; *b* position C; *c* position F

7 Images (TEM) of typical positions in RZ shown in Fig. 3

precipitation of few Cr carbides in the RZ would not cause obvious Cr depletion and result in the degradation of the corrosion resistance of austenite stainless steel.

Acknowledgement

The work was funded by the 'Innovative Nuclear Research and Development Program' of the Ministry of Education, Culture, Sports, Science and Technology, Japan.

References

1. W. M. Thomas, E. D. Nicholas, J. C. Needham, M. G. Murch, P. Temple-Smith and C. J. Dawes: 'Friction stir welding', International Patent Application No. PCT/GB92/02203 and Great Britain Patent Application No. 9125978·8, 1991.
2. R. S. Mishra and Z. Y. Ma: 'Friction stir welding and processing', *Mater. Sci. Eng. R*, 2005, **R50**, 1–78.
3. R. Nandan, T. DebRoy and H. Bhadeshia: 'Recent advances in friction-stir welding – process, weldment structure and properties', *Prog. Mater. Sci.*, 2008, **53**, 980–1023.
4. P. L. Threadgill, A. J. Leonard, H. R. Shercliff and P. J. Withers: 'Friction stir welding of aluminium alloys', *Int. Mater. Rev.*, 2009, **54**, 49–93.
5. H. Bhadeshia and T. DebRoy: 'Critical assessment: friction stir welding of steels', *Sci. Technol. Weld. Join.*, 2009, **14**, 193–196.
6. A. Oosterkamp, L. D. Oosterkamp and A. Nordeide: '"Kissing bond" phenomena in solid-state welds of aluminum alloys', *Weld. J.*, 2004, **83**, 225S–231S.
7. H. B. Chen, K. Yan, T. Lin, S. B. Chen, C. Y. Jiang and Y. Zhao: 'The investigation of typical welding defects for 5456 aluminum alloy friction stir welds', *Mater. Sci. Eng. A*, 2006, **A433**, 64–69.
8. H. Zhang, S. B. Lin, L. Wu, J. C. Feng and S. L. Ma: 'Defects formation procedure and mathematic model for defect free friction stir welding of magnesium alloy', *Mater. Des.*, 2006, **27**, 805–809.
9. R. Crawford, G. E. Cook, A. M. Strauss, D. A. Hartman and M. A. Stremler: 'Experimental defect analysis and force prediction simulation of high weld pitch friction stir welding', *Sci. Technol. Weld. Join.*, 2006, **11**, 657–665.
10. Y. G. Kim, H. Fujii, T. Tsumura, T. Komazaki and K. Nakata: 'Three defect types in friction stir welding of aluminum die casting alloy', *Mater. Sci. Eng. A*, 2006, **A415**, 250–254.
11. W. J. Arbegast: 'A flow-partitioned deformation zone model for defect formation during friction stir welding', *Scr. Mater.*, 2008, **58**, 372–376.
12. T. L. Dickerson and J. Przydatek: 'Fatigue of friction stir welds in aluminium alloys that contain root flaws', *Int. J. Fatigue*, 2003, **25**, 1399–1409.
13. H. J. Liu, Y. C. Chen and J. C. Feng: 'Effect of zigzag line on the mechanical properties of friction stir welded joints of an Al–Cu alloy', *Scr. Mater.*, 2006, **55**, 231–234.
14. C. Z. Zhou, X. Q. Yang and G. H. Luan: 'Effect of kissing bond on fatigue behavior of friction stir welds on Al 5083 alloy', *J. Mater. Sci.*, 2006, **41**, 2771–2777.
15. C. Z. Zhou, X. Q. Yang and G. H. Luan: 'Effect of root flaws on the fatigue property of friction stir welds in 2024-T3 aluminum alloys', *Mater. Sci. Eng. A*, 2006, **A418**, 155–160.
16. C. Z. Zhou, X. Q. Yang and G. H. Luan: 'Effect of oxide array on the fatigue property of friction stir welds', *Scr. Mater.*, 2006, **54**, 1515–1520.
17. S. S. Di, X. Q. Yang, D. P. Fang and G. H. Luan: 'The influence of zigzag-curve defect on the fatigue properties of friction stir welds in 7075-T6 Al alloy', *Mater. Chem. Phys.*, 2007, **104**, 244–248.
18. W. M. Thomas, H. G. Pisarski, I. M. Norris, D. J. Marks and J. C. Godden: 'An investigation of through-hole impact testing of weld root imperfections in friction stir welded 12 percent chromium alloy steel', *Proc. Inst. Mech. Eng. B*, 2008, **222B**, 1043–1054.
19. H. J. Liu and H. J. Zhang: 'Repair welding process of friction stir welding groove defect', *Trans. Nonferrous Met. Soc. China*, 2009, **19**, 563–567.
20. R. J. Ding and A. Oelgoetzp: 'The hydraulic controlled auto-adjustable pin tool for friction stir welding', US Patent 5,893,507, 1996.
21. C. D. Allen and W. J. Arbegast: 'Evaluation of friction spot welds in aluminium alloys', SAE technical paper no. 2005-01-1252, SAE International, Warrendale, PA, USA, 2005.
22. Y. Uematsu, K. Tokaji, Y. Tozaki, T. Kutita and S. Murata: 'Effect of re-filling probe hole on tensile failure and fatigue behaviour of friction stir spot welded joints in Al–Mg–Si alloy', *Int. J. Fatigue*, 2008, **30**, 1956–1966.
23. S. B. Dunkerton, D. E. Nicholas and P. D. Sketchley: 'Repairing defective metal workpiece – by friction welding with a metal plug', Great Britain Patent Application No. 9125978, 1991.
24. W. M. Thomas and P. Temple-Smith: 'Friction plug extrusion for solid-phase welding thick plates – by relatively moving consumable member and bore in substrate while urging them together to generate frictional heat to plasticise member', Great Britain Patent Application No. 2306365, 1997.
25. J. Unfried S, M. T. P. Paes, T. F. C. Hermenegildo, F. L. Bastian and A. J. Ramirez: 'Study of microstructural evolution of friction taper plug welded joints of C–Mn steels', *Sci. Technol. Weld. Join.*, 2010, **15**, 506–513.
26. P. J. Hartley: 'Friction plug weld repair for the space shuttle external tank', *Weld. Met. Fab.*, 2002, **9**, 6–8.
27. Y. X. Huang, B. Han, Y. Tian, H. J. Liu, S. X. Lv, J. C. Feng, J. S. Leng and Y. Li: 'New technique of filling friction stir welding', *Sci. Technol. Weld. Join.*, 2011, **16**, 497–501.
28. Y. X. Huang, B. Han, S. X. Lv, J. C. Feng, H. J. Liu, J. S. Leng and Y. Li: 'Interface behaviours and mechanical properties of filling friction stir weld joining AA 2219', *Sci. Technol. Weld. Join.*, 2012, **17**, 225–230.
29. Y. C. Chen, H. Fujii, T. Tsumura, Y. Kitagawa, K. Nakata, K. Ikeuchi, K. Matsubayashi, Y. Michishita, Y. Fujiya and J. Katoh: 'Friction stir processing of 316L stainless steel plate', *Sci. Technol. Weld. Join.*, 2009, **14**, 197–201.
30. Y. C. Chen, H. Fujii, T. Tsumura, Y. Kitagawa, K. Nakata, K. Ikeuchi, K. Matsubayashi, Y. Michishita, Y. Fujiya and J. Katoh: 'Banded structure and its distribution in friction stir processing of 316L austenitic stainless steel', *J. Nucl. Mater.*, 2012, **420**, 497–500.
31. S. H. C. Park, Y. S. Sato, H. Kokawa, K. Okamoto, S. Hirano and M. Inagaki: 'Rapid formation of the sigma phase in 304 stainless steel during friction stir welding', *Scr. Mater.*, 2003, **49**, 1175–1180.
32. Y. S. Sato, N. Harayama, H. Kokawa, H. Inoue, Y. Tadokoro and S. Tsuge: 'Evaluation of microstructure and properties in friction stir welded superaustenitic stainless steel', *Sci. Technol. Weld. Join.*, 2009, **14**, 202–209.
33. S. H. C. Park, Y. S. Sato, H. Kokawa, K. Okamoto, S. Hirano and M. Inagaki: 'Corrosion resistance of friction stir welded 304 stainless steel', *Scr. Mater.*, 2004, **51**, 101–105.
34. M. Schwind, J. Kallqvist, J. O. Nilsson, J. Agren and H. O. Andren: 'σ-phase precipitation in stabilised austenitic stainless steels', *Acta Mater.*, 2000, **48**, 2473–2481.
35. R. A. Farrar: 'Microstructure and phase transformations in duplex 316 submerged arc weld metal, an ageing study at 700°C', *J. Mater. Sci.*, 1985, **20**, 4215–4231.
36. Y. S. Sato and H. Kokawa: 'Preferential precipitation site of sigma phase in duplex stainless steel weld metal', *Scr. Mater.*, 1999, **40**, 659–663.
37. S. H. C. Park, Y. S. Sato, H. Kokawa, K. Okamoto, S. Hirano and M. Inagaki: 'Microstructural characterisation of stir zone containing residual ferrite in friction stir welded 304 austenitic stainless steel', *Sci. Technol. Weld. Join.*, 2005, **10**, 550–556.